



Influence of Surface Irregularities on the Expected Boundary-Layer Transition Location on Hybrid Laminar Flow Control Wings

Juan Alberto Franco Sumariva^(✉), Alexander Theiss, and Stefan Hein

Institut für Aerodynamik und Strömungstechnik, DLR,
Bunsenstraße 10, 37073 Göttingen, Germany
Juan.Franco@dlr.de

Abstract. Hybrid laminar flow control (HLFC) is a promising concept to reduce the viscous drag on aircraft wings by shifting the expected laminar-turbulent transition (LTT) location downstream. However, the structural joint between the leading edge suction panel and the wing box can diminish this desirable shift in LTT location and thus reduce the efficiency of the HLFC system. This paper introduces a toolchain, which allows to numerically quantify the detrimental effects of two-dimensional surface irregularities for transonic HLFC swept wings at free-flight Reynolds numbers. A backward-facing step and two different gaps are studied, which resemble possible structural joint geometries currently considered within the HLFC-WIN project. The stability analysis performed with the Adaptive Harmonic Linearized Navier-Stokes (AHLNS) approach reveals that none of the three irregularities affects the expected LTT location, suggesting that there might be some potential to relax the surface tolerances initially specified in the HLFC-WIN project using classical criteria.

Keywords: Transition · Surface irregularity · HLFC · AHLNS · PSE

1 Introduction

Hybrid laminar flow control (HLFC) wings have captured the interest of several research projects, in particular the HLFC-WIN project [1], because of the potential of suction for reducing drag on commercial aircraft [2]. This reduction in drag is mainly due to the impact on laminar-turbulent transition (LTT), extending the region along the wings where the flow remains laminar. In such circumstances, the growth of flow instabilities (e.g. Tollmien-Schlichting (TS) waves or crossflow (CF) vortices), might trigger the LTT. Typically, on HLFC wings, suction is applied only in the leading edge region (before the front spar). The flow suction modifies the boundary-layer (BL) profiles in such a way that the growth of the above-mentioned flow instabilities is delayed.

However, the joint between the leading edge suction panel and the wing box may introduce surface irregularities (e.g. backward/forward-facing steps

(BFS/FFS), gaps, etc.) that might enhance the spatial development of those flow instabilities and, therefore, reduce the potential benefit of the suction system [3]. For this reason, it is crucial during the design process to quantify the influence of such surface irregularities in terms of BL instability.

Techniques like Parabolized Stability Equations (PSE) [4] are not suited for BL instability analysis in the vicinity of those surface irregularities: its formulation assumes that streamwise variations of base flow and disturbances quantities are small (with respect to surface-normal variations). On the other hand, approaches like Linearized Navier-Stokes (LNS), Harmonic LNS (HLNS), and Direct Numerical Simulation (DNS) do not impose any assumption regarding the nature of the convective instabilities in streamwise direction. This fact implies that the required numerical resources increase significantly. Alternatively, the Adaptive Harmonic LNS (AHLNS) equations [5] can also handle these large streamwise gradients using a fully-elliptic system of equations (similar to DNS). In contrast, the AHLNS formulation assumes a *wave-like* character of the instabilities (as in PSE), leading to a significant reduction in the number of streamwise grid points required compared with LNS, HLNS, or DNS computations.

Alternatively to the above described numerical approaches, it is very common in the industry to use the criteria defined in the work of Nenni and Gluyas [6], who gave a critical Reynolds number for certain types of surface irregularities, based on incoming flow conditions and geometrical dimensions of the surface irregularity only. The criteria were established for a particular flow condition and airfoil geometry (The X21-wing). Therefore, although the use of the Nenni and Gluyas criteria provides a rapid estimation of the maximum allowable dimensions for a surface irregularity, the range of validity of such estimation is very limited.

The present paper provides a systematic procedure for the study of the effect of 2D surface irregularities (in particular, a BFS and two different gaps) on the expected LTT location for HLFC wings at transonic flow conditions using the recently developed AHLNS approach. To the authors' knowledge, there is no similar work published from numerical computations.

2 Methodology

This section outlines the numerical methods used to obtain the steady laminar base flow and the BL instability characteristics affected by different surface irregularities located at the joint between the leading edge suction panel and the wing box on an HLFC wing.

2.1 Reference Design and Base Flow Computation

The original fully three-dimensional (3D) wing geometry corresponds to a design used in the HLFC-WIN project [1] equipped with a leading edge suction panel that reaches up to about 20% of the chord on the upper side of the wing. The base flow has been obtained numerically using the DLR TAU code, a compressible

unstructured and Reynolds-averaged Navier-Stokes code for external flows [10] and was kindly made available by Martin Kruse (DLR).

Above reference flow for the nominally smooth 3D wing geometry with suction had been computed using the following approach. First, a TAU simulation was performed for a wing surface without any prescribed suction rates on the suction panel. However, the impact of the suctioned BL flow was considered within the employed transition prediction toolchain. Based on the TAU-computed pressure distribution without suction, a laminar base flow including suction was generated with the BL code COCO [7] for several line-in-flight cuts. Subsequently, the growth of TS waves and CF vortices was investigated utilizing the local incompressible stability theory within the LILO code [8] and the transition location prescribed in the TAU computations was iteratively updated based on N -factor results using the N_{CF} - N_{TS} transition prediction strategy.

The described procedure (coupling of TAU+COCO+LILO) is, however, not suited to study the impact of surface imperfections on the growth of BL instabilities since no laminar base flows can be generated with the BL code COCO including surface irregularities like steps and gaps. Furthermore, the surface imperfections induce streamwise gradients into the flow, which are not considered in the local stability theory. For this reason, the base flow computation including surface irregularity and suction is completely performed with the TAU code, and the BL stability properties are investigated according to the compressible non-local theory employing the PSE/AHLNS framework, which is briefly outlined in Sect. 2.4.

Moreover, the computational demands for the entire 3D flow field simulation, including the joint between the leading edge suction panel and the wing box, are excessively high. In order to ease the computational effort and thus study various joint geometries and assess their impact on the BL instability characteristics, the flow field of the original 3D wing at a selected line-in-flight cut is approximated by an infinite swept-wing 2.5D flow with similar BL properties.

2.2 Infinite Swept-Wing Approximation

The selected line-in-flight cut is located at around 2/3 of the wingspan because this section has the most conical flow condition compared to other spanwise cuts. To ensure that the BL and instability characteristics in the selected cut are comparable to the original 3D flow field, the same toolchain is utilized as for the reference case without surface irregularity (i.e. BL computation including suction based on the pressure distribution obtained from a TAU simulation without suction, and subsequent incompressible, local instability analysis using LILO together with the N_{CF} - N_{TS} transition prediction strategy).

The reference pressure distribution is approximated in a parameter study in which the freestream Mach number Ma_∞ , the angle of attack α , and the sideslip angle γ were varied in the 2.5D computation. In contrast, the airfoil geometry and suction distribution remained unchanged. Moreover, the transition location predicted for the 3D reference configuration in the selected slice ($x_{tr}/c \approx 0.54$) is also prescribed as the transition location in the 2.5D TAU simulation.

The parameter combination that best approximates both the pressure distribution and the spatial evolution of the convective instabilities is $\alpha = 2.6^\circ$, $Ma_\infty = 0.78$, and $\gamma = 14^\circ$ (see Fig. 1).

The depicted N -factor curves in Fig. 1b are envelopes of n -factor curves representing different frequencies at a zero-degree wave angle (TS) or various total wavelengths at zero frequency (CF). The n -factor is a measure of the accumulated growth of a disturbance and is defined as $n(x) = \ln(A(x)/A_0)$, where A_0 denotes the maximum amplitude, in the wall-normal direction, of the streamwise velocity component of the corresponding instability mode at the streamwise position where the disturbance starts to grow. The n -factor is set to zero if, during the calculation, the value of A becomes smaller than A_0 .

Note that the CF instability is not amplified in the 2.5D flow field. However, in the 3D reference case at the joint location and the subsequent chord section, the TS waves are most amplified and likely to dominate the transition scenario in the selected line-in-flight cut. Therefore, in the present study, the instability analysis solely focuses on the spatial development of TS waves.

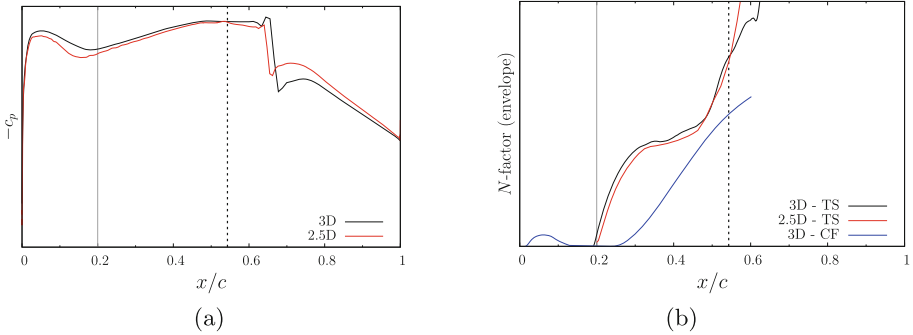


Fig. 1. Comparison of the original 3D flow solution at the selected line-in-flight cut with the approximated 2.5D solution in terms of (a) pressure distribution and (b) instability results. The vertical grey line represents the joint position, while the black dashed line indicates the prescribed LTT location in the base flow TAU computations. The 3D reference data have been provided by Martin Kruse (DLR).

2.3 Surface Irregularity

Once the infinite swept-wing 2.5D flow is defined (see Sect. 2.2), it is feasible to incorporate the joint geometry into the two-dimensional (2D) airfoil shape. DLR's structured grid generator MEGACADS [11] is used for this task. Three examples of irregularities are considered for representing the 2D geometry of the joint between the leading edge suction panel and the wing box. The BFS and the two gaps of different width resemble possible structural joint concepts currently considered within the HLFC-WIN project, and the choice of their geometrical dimensions was motivated by simple criteria similar to the classical Nenni and Glyvas criteria. Their actual geometrical characteristics are given in Table 1.

The geometrical shape is shown in the flow field visualizations in Fig. 2. The position of the surface irregularities is fixed to 20% of the chord for all cases considered.

2.4 Instability Analysis

The Adaptive Harmonic Linearized Navier-Stokes (AHLNS) approach [5], in combination with the Parabolized Stability equations (PSE) [4], offers the most efficient way to compute the effect of surface irregularities on the spatial development of convective instabilities, e.g. TS waves and CF vortices, in terms of n -factor curves. The PSE are applied far from the location of the surface irregularity, where the streamwise variations of the base flow quantities remain small (w.r.t. wall-normal gradients). The AHLNS methodology is used in the vicinity of the irregularity, where the assumption of small variations in streamwise direction of the base flow variables is no longer valid. The efficiency of the AHLNS approach, in comparison with other standard methodologies as HLNS or DNS, lies in the *wave-like* character assumed for describing the convective instabilities, in a similar fashion as PSE. This assumption significantly reduces the number of streamwise grid points required in comparison with DNS computations [5], allowing parametric studies for transonic wings at high Reynolds numbers. An example of the combination of PSE and AHLNS for a parametric study of the effect of a surface irregularity in a compressible flow at a high Reynolds number can be found in the work of Franco et al. [9].

3 Results

3.1 Base Flow Computations

Figure 2 shows the contours of Mach number and two-dimensional streamlines for the three joints chosen. Figure 3 displays the non-dimensional pressure distribution p_{wall} along the airfoil's suction side for all cases studied here. Moreover, the pressure distribution for the clean configuration (label “*No irregularity*”) has been included as reference. The pressure is made non-dimensional by twice the incoming dynamic pressure, i.e. $\rho_\infty (U_\infty)^2$.

The presence of the backward-facing step introduces an elongated recirculation bubble (see Fig. 2a) with an extension in streamwise direction significantly

Table 1. Surface irregularities (joint geometry) considered in the present work

| Name | Type | Depth [mm] | Width [mm] |
|-------|----------------------|------------|------------|
| BFS | Backward-facing step | 0.2 | – |
| Gap 1 | Gap | 0.8 | 1 |
| Gap 2 | Gap | 0.8 | 3 |

larger than the step height. Regarding the pressure distribution at the wall p_{wall} (Fig. 3), the existence of the BFS is substantially more influential than any of the other two irregularities. Clearly, the pressure distribution for the BFS case deviates from the clean configuration in a much larger extension than the other two gaps considered here. This fact suggests that the BFS might affect the spatial development of the incoming TS waves more significantly than the two gap cases.

On the other hand, it is interesting to notice that the recirculation flow due to the presence of a gap (see Figs. 2b and 2c) does not deflect significantly the streamlines coming upstream of the gap. This fact is confirmed by checking the pressure distribution at the wall p_{wall} (Fig. 3) for both gap cases. The pressure distribution deviates from the clean configuration case only in the close vicinity of the gap location. It is also important to mention the peak in the pressure distribution that appears at the location of each gap. They represent the rapid changes in streamwise direction of the base flow magnitudes provoked by the geometry of the gap and justify the necessity of using the AHLNS approach for the subsequent stability analysis (as it was explained in Sect. 2.4).

3.2 N -Factor Curves

A preliminary instability analysis study (not included in the present paper) for the 2.5D clean configuration (i.e. no geometrical joint incorporated into the shape of the airfoil) was done using the PSE code NOLOT [4] for TS instabilities. This study indicated that the most relevant n -factor curves (each one obtained for a particular spanwise wavenumber β and frequency f) were found in the parametric space $\beta \in [200\text{--}400] \text{ m}^{-1}$ and $f \in [1000\text{--}6000] \text{ Hz}$.

The N -factor curve, envelope of all particular n -factor curves computed in the above defined parametric space (β, f) , is depicted in Fig. 4 with the label *No irregularity* for the case where the joint does not introduce any surface irregularity. The small increase present for the *No irregularity* case at $x/c \approx 0.20$ is due to the sudden change in boundary conditions for the base flow: from a given suction flow rate at the leading-edge suction panel to a zero-flow rate at the wing box. In the same plot, the N -factor curves for the three joint geometries considered in this study are also included. Clearly, the BFS is the surface irregularity that introduces a larger distortion in the spatial development of the incoming TS waves. This result agrees with the explanation provided for the base flow in Sect. 3.1. However, in the proximity where the transition was fixed for the steady base flow computations (i.e. $x/c \approx 0.54$, see Sect. 2.2), the amplification curves for the BFS and the clean configuration tend to collapse. This result might imply that the BFS considered here does not change the expected transition location significantly (with respect to the expected LTT location of the clean configuration).

For the two gap cases (Gap 1 and Gap 2), their influence on the incoming TS waves is manifestly smaller than for the BFS case. For the Gap 1, the N -factor envelope curve almost overlaps with the amplification curve of the clean configuration along the whole profile. Therefore, it can be concluded that, in terms

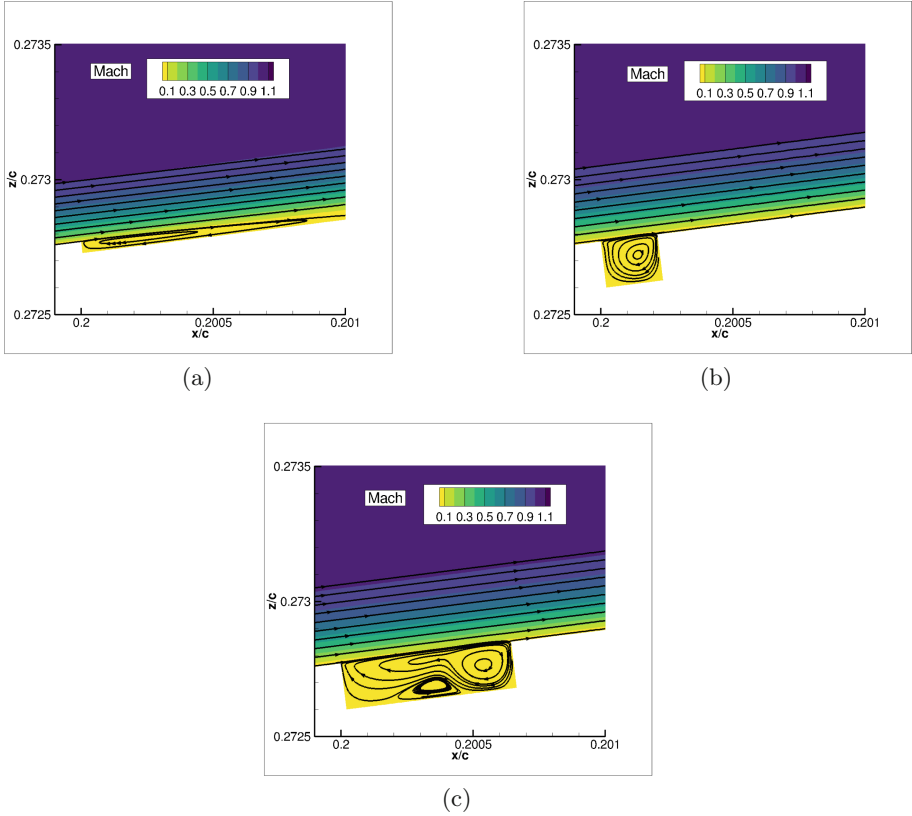


Fig. 2. Steady laminar base flow results. Mach number contours and two-dimensional streamlines for cases (a) BFS; (b) Gap 1; (c) Gap 2.

of stability analysis, the presence of such irregularity is negligible. For the Gap 2, although its width is three times larger than the Gap 1 width, the situation is similar. The N -factor envelope curve deviates from the clean configuration case only in a very small region downstream of the gap location and, after that, both amplification curves coincide. Consequently, it can also be stated that the influence of Gap 2, in terms of expected transition location, is not significant.

Finally, Fig. 5 shows the spatial evolution of an incoming TS wave of frequency $f = 2000$ Hz and spanwise wavenumber $\beta = 200 \text{ m}^{-1}$ passing along the Gap 2 case. The body-attached coordinates are defined as: s represents the arc-length along the airfoil surface (with origin at the leading edge), and η holds for the surface-normal coordinate. For this particular instability, the streamwise wave length is about 6 cm, while the gap width for the surface irregularity is 3 mm

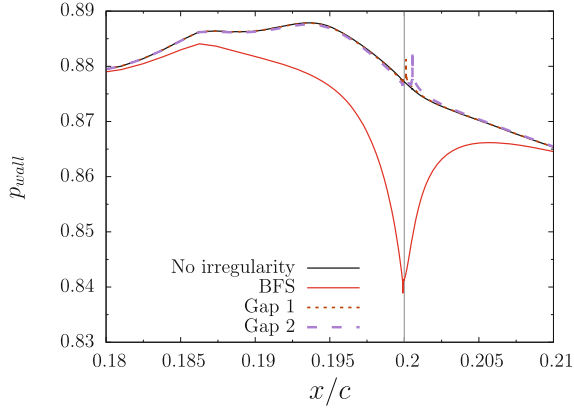


Fig. 3. Steady laminar base flow results. Non-dimensional pressure distribution at the wall p_{wall} . The vertical grey line represents the location of the joint between the leading edge suction panel and the wing box.

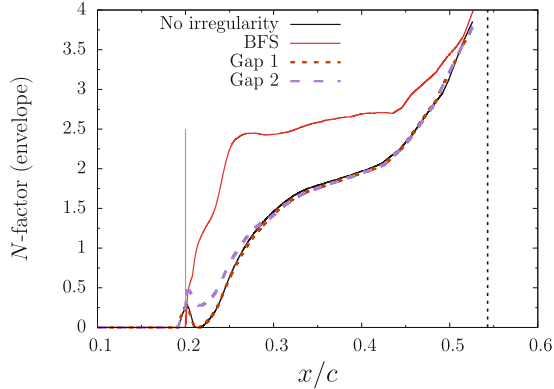


Fig. 4. N -factor envelope curves for all joints considered in the present work. The clean configuration (*No irregularity*) has been included as reference. The vertical grey line represents the location of the joint between the leading edge suction panel and the wing box. The vertical black dashed line indicates the prescribed LTT location in the base flow TAU computations.

(see Table 1). This large difference in streamwise length scales between surface irregularity and instability mode also helps to understand the small influence of the two gap cases considered regarding the expected transition location.

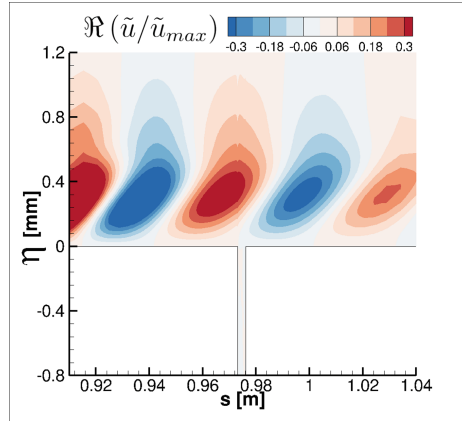


Fig. 5. Real part of the streamwise velocity disturbance \tilde{u} for an incoming TS wave of frequency $f = 2000$ Hz and spanwise wavenumber $\beta = 200 \text{ m}^{-1}$ at an arbitrary instant of time for the Gap 2 case. Body-attached coordinates (s, η) [axes are not to scale].

4 Conclusions

The effect of different two-dimensional surface irregularities on the expected laminar-turbulent transition location on a realistic HLFC wing has been analyzed by means of the AHLNS methodology for the first time. The combined effect of infinite swept-wing configuration, airfoil geometry, transonic flow conditions, and suction represents a qualitative step forward with respect to previous applications of the AHLNS approach, where only zero-pressure gradient and flat-plate configurations were considered. It could be demonstrated that, with the toolchain established within the HLFC-WIN project, it is now possible to take into account the actual laminar flow field and the respective linear stability characteristics when assessing the effect of surface irregularities on laminar-turbulent transition for such configurations, in contrast to the simple criteria of Nenni and Gluyas based on the freestream conditions and a single geometrical dimension only. Thus, after a successful validation against suitable experimental data, the present approach may prove to be much more reliable when used for the specification of surface allowables compared to the simple but much faster classical criteria.

The three surface irregularities studied in the present paper resemble possible structural joint concepts currently considered within the HLFC-WIN project. The choice of their geometrical dimensions was motivated by the maximum tolerances estimated by simple criteria similar to the classical Nenni and Gluyas criteria. For the freestream conditions and suction distribution considered, none of the surface irregularities studied here are expected to have an influence on the transition location. However, the BFS caused a significant rise in the N -factor envelope in the immediate downstream vicinity of the irregularity. Therefore, for flow conditions at which the N -factors at the BFS are higher already, the

situation may be different. Hence, further studies at other flow conditions, other dimensions of the surface irregularities, and other chord positions of the joint should be performed in order to check whether the surface requirements for the present HLFC-WIN configuration can indeed be relaxed compared to the rather challenging constraints that were originally imposed using the simple criteria. Moreover, the AHLNS approach is not limited to ideally sharp rectangular geometries, as it was demonstrated in Franco et al. [9], and could also be used e.g. for gap cases with a certain vertical offset between the upstream and downstream edges of the gap. Thus, the present approach can be used to study more realistic joint configurations not covered by the classical criteria for single rectangular FFS/BFS and simple rectangular gaps.

Acknowledgments. The authors would like to thank Martin Kruse (DLR) for providing the complete 3D base flow computation of the HLFC wing and the TAU version for the base flow simulations including suction, and Thomas Haase (DLR) for his careful review of our manuscript and his insightful comments. We also acknowledge valuable contributions from all partners of the HLFC-WIN consortium: Aernnova, DLR, Onera, Sonaca and Airbus. This project has received funding from the Clean Sky 2 Joint Undertaking (JU) under grant agreement No. 945583. The JU receives support from the European Union's Horizon 2020 research and innovation programme and the Clean Sky 2 JU members other than the Union. The results, opinions, conclusions, etc. presented in this work are those of the author(s) only and do not necessarily represent the position of the JU; the JU is not responsible for any use made of the information contained herein.

References

1. HLFC-WIN project. <https://www.hlfc-win.eu/>
2. Reneaux, J.: Overview on drag reduction technologies for civil transport aircraft. In: ECCOMAS (2004)
3. Methel, J., Forte, M., Vermeersch, O., Casalis, G.: An experimental study on the effects of two-dimensional positive surface defects on the laminar-turbulent transition of a sucked boundary layer. *Exp. Fluids* **60**, 94 (2019)
4. Hein, S., Bertolotti, F.P., Simen, M., Hanifi, A., Henningson, D.: Linear nonlocal instability analysis - the linear NOLOT code. Internal Report No. DLR IB 223-94 A56 (1995)
5. Franco Sumariva, J.A., Hein, S.: Adaptive harmonic linearized Navier-Stokes equations used for boundary-layer instability analysis in the presence of large streamwise gradients. In: AIAA Paper 2018-1548 (2018)
6. Nenni, J.P., Gluyas, G.L.: Aerodynamic design and analysis of an LFC surface. *Astron. Aeronaut.* **4**, 52-57 (1966)
7. Schrauf, G.: COCO - a program to compute velocity and temperature profiles for local and nonlocal stability analysis of compressible, conical boundary layers with suction. ZARM Technik report (1998)
8. Schrauf, G.: LILO 2.1 user's guide and tutorial. GSSC Technical report 6, originally issued Sep. 2004, modified for Version 2.1 (2006)
9. Franco Sumariva, J.A., Hein, S., Valero, E.: On the influence of two-dimensional hump roughness on laminar-turbulent transition. *Phys. Fluids* **32**, 034102 (2020)

10. TAU-Code User Guide. DLR. v.2017.1.0 (2017)
11. Brodersen, O., Ronzheimer, A., Ziegler, R., Kunert, T., Wild, J., Hepperle, M.: Aerodynamic Applications using MegaCads. In: 6th International Conference on Numerical Grid Generation (1998)